Heat and Technology
Vol. 32, n. 1-2, 2014

3D CFD EXERGY ANALYSIS OF THE PERFORMANCE OF A COUNTER FLOW VORTEX TUBE

S. E. Rafiee*, M. M. Sadeghiazad

Department of Mechanical Engineering, Urmia University of Technology, Urmia, Iran.

ABSTRACT

In this numerical study, exergy analysis of a Ranque-Hilsch vortex tube (RHVT) has been investigated. The three-dimensional (3D) computational fluid dynamic (CFD) model which is used in this study is a steady axisymmetric model that employs two turbulence models (standard k-ε and standard k-ω) to perform the computation procedure of results. All of these computations are based on the second-order numerical schemes. The curves of exergy performance such as inlet exergy, exergy of cold and hot outlet, lost exergy and exergy efficiency have been achieved for the present vortex tube. These curves have been validated with the experimental data and have shown good agreement. In this paper, variation of exergy in the cold and hot exit has been predicted as a function of cold mass fraction and the behaviors of obtained curves have been discussed. In addition, variation of temperature and pressure in the cold and hot exhaust has been presented as a function of cold mass fraction. More ever the comparison between two turbulence model results has been obtained in different fields such as exergy, pressure and temperature.

Keywords: Exergy analysis; Ranque-Hilsch vortex tube (RHVT); Three-dimensional (3D); Computational fluid dynamic (CFD) model; Turbulence models

1. INTRODUCTION

Vortex tube is a device with an ordinary geometry that produces two gas stream containing cold and hot gas stream from compressed inlet gas. When pressured gas is injected into the vortex chamber tangentially via the inlet nozzles a powerful rotational flow field is established. The gas is expanded and cooled when it swirls to the center of the chamber. At the hot exhaust the gas escapes with a higher temperature, while at the cold exhaust, the gas has a lower temperature compared to the pressured inlet gas. A Ranque-Hilsch vortex tube (RHVT) has the following interests compared to the normal commercial refrigeration device: Simple, no moving parts, no electricity or chemicals, small and light weight, low cost, maintenance free, instant cold air and durable. But its low thermal efficiency is a principal limiting factor for its usage. Determining this efficiency is useful to improve and optimize the vortex tube parameters. Vortex tube was first discovered by Ranque in 1932 when he was studying processes in a dust separation cyclone [1], and the German physicist Rudolf Hilsch improved the design [2]. Vortex tubes are classified into two groups according to their flow directions: counter flow RHVTs, as seen in Fig. 1 and parallel flow RHVTs as shown in Fig. 2. In this investigation a counter flow RHVT has been used.

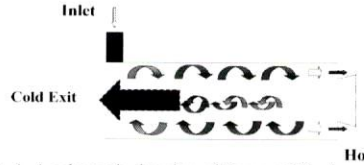

Fig. 1. A schematic drawing of Ranque-Hilsch vortex tube

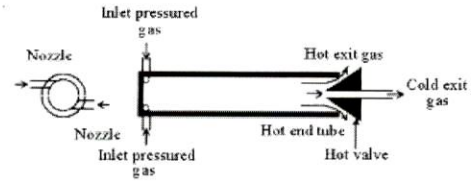

Fig. 2. The schematic representation of a parallel flow vortex tube principle (Eiamsa-ard and Promvonge, 2007) [28]

Hot and cold flows in parallel flow vortex tube leave from the vortex tube in the same directions. The vortex tube has been a subject of many studies. Some of these investigations are briefly mentioned below:
Rafiee and Rahimi [3] performed an experimental work on convergence ratio of nozzles and in their work a three dimensional computational fluid dynamic model was introduced as a predictive tools to obtain the maximum cold temperature difference. Also they proved that energy separation procedure inside the vortex tube can be improved by using convergent nozzle. Ahlborn and Gordon [4] explained an embedded secondary circulation and Stephan *et al.* [5] proposed the constitution of Gortler vortices on the inside wall of the vortex tube that drive the fluid motion. Rafiee and Sadeghi [6] performed an experimental and numerical work on cone length of control valve of vortex tube. Skye *et al* [7] employed a model similar to that of Aljuwayhel. Pourmahmoud et al [8] investigated numerically the effect of convergent nozzle in flow patterns. Rafiee et.al [9] numerically investigated the effect of working tube radius

on vortex tube performance and the optimum working tube radius has been determined. Pourmahmoud and Rafiee [10] also performed a numerical study on working fluid importance in vortex tube applications and their study showed, CO_2 is better than O_2, N_2 and air. Chang H Sohn *et al* [11] conducted a visualization experiment using surface tracing method to investigation the internal flow phenomena and to illustrate the stagnation position within a vortex tube. Ameri *et al* [12] and Eisma *et al* [13] carried out a numerical study to understand the flow field and temperature separation phenomenon. Also some studies have been performed to use vortex tube as refrigeration device, instead of the usual refrigeration systems, for example, Alka Bani Agrawal; Vipin Shrivastava [14], and Jayaraman, Senthil Kumar [15]. Volkan Kirmaci [16] used Taguchi method to optimize and simulate the number of nozzles of vortex tube. In general definition, exergy is the maximal work, attainable in given source state with any generalized friction. In closed system energy is conserved but exergy is destroyed due to generalized friction. In the thermodynamics the exergy of a system is a maximum useful work possible during a procedure that brings the system into balance with a heat reservoir.The units of exergy are the same as for energy or heat, such as kilocalories, joules, BTUs, etc. Some of the exergy investigations are briefly mentioned below. Dincer *et al* [17] carried out an experimental study about exergy analysis of the performance of a counter flow Ranque-Hilsch vortex tube with regard to nozzle cross-section area. Ceylan *et al* [18] performed an exergy research for timber dryer assisted heat pump. Kirmaci [19] carried out exergy analysis of a counter flow Ranque-Hilsch vortex tube with different nozzle numbers at various inlet pressures. This study was performed using O_2 and air as pressured inlet gas. Also in other fields some works have been done, for example, Ozgener and Hepbasli [20], Saidur *et al* [21], Esen *et al* [22]. A valuable work was done to analyze the isotope separation using vortex tubes by Lorenzini *et al.* [23].

THEORETICAL EXERGY ANALYSIS FOR VORTEX TUBE

The total exergy of a system can be written as [24]:

$$\sum \dot{E} = \dot{E}_{PH} + \dot{E}_{KN} + \dot{E}_{PT} + \dot{E}_{CH} \quad (1)$$

In this equation, $\sum \dot{E}$, $\dot{E}_{PH}$, $\dot{E}_{KN}$, $\dot{E}_{PT}$ and $\dot{E}_{CH}$ represent the total exergy, physical exergy, kinetic exergy, potential exergy and chemical exergy of a system respectively. The physical exergy can be computed by following equation [17]:

$$\dot{E}_{PH} = \dot{m}[C_p(T - T_0) - T_0(C_p \ln\frac{T}{T_0} - R \ln\frac{P}{P_0})] \quad (2)$$

Where, in this equation, $\dot{m}$ and C_p are mass flow rate and specific heat of a system respectively. Also T is temperature at any instant, T_0 is the initial temperature, P is pressure at any instant, P_0 is the initial pressure and R is a gas constant. The initial temperature and pressure are assumed as T_0 = 294.2 K and P_0 = 100 kPa, reflectively.

The kinetic exergy and the potential exergy [25] can be given as:

$$\dot{E}_{KN} = \frac{\dot{m}v^2}{2} \quad (3)$$

$$\dot{E}_{PT} = \dot{m}gz \quad (4)$$

In equation 3, v is velocity of the flow and in equation 4; g is gravitational acceleration and z in this case can be defined as height difference between the position of hot outlet and inlet of vortex tube. In this study we need some assumption that can be given as follow.

i. The governing conditions in this case can be defined as steady state.

ii. Friction effect in this case (RHVT) is neglected.

iii. The conditions of flow in RHVT are adiabatic.

iv. The fluid in this study can be assumed as ideal gas.

v. No chemical event is considered in RHVT system.

vi. According to option (v), there is no chemical event in RHVT, therefore, $\dot{E}_{CH}$ or chemical exergy can be neglected. Actually the potential exergy or $\dot{E}_{PT}$ can be assumed to be zero because z or height difference between hot outlet and inlet of vortex tube is so small. So the equation (1) can be given as [26].

$$\sum \dot{E}_i = \dot{E}_{i,PH} + \dot{E}_{i,KN} \quad (5)$$

Where, $\dot{E}_{i,PH}$, $\dot{E}_{i,KN}$ are the inlet physical exergy and the inlet kinetic exergy of the system respectively. Therefore:

$$\sum \dot{E}_{PH} = \dot{m}_i[C_p(T_i - T_0) - T_0(C_p \ln\frac{T_i}{T_0} - R \ln\frac{P_i}{P_0})] + \frac{\dot{m}_i v_i^2}{2} \quad (6)$$

Where T_i is the inlet temperature, P_i is the inlet pressure, $\dot{m}_i$ is the mass flow inlet and v_i is the velocity of the pressured inlet gas. Also there is the total exergy outlet that can be defined as [26]:

$$\sum \dot{E}_o = \dot{E}_{o,hot} + \dot{E}_{o,cold} \quad (7)$$

Where:

$$\sum \dot{E}_{o,hot} = \dot{m}_{hot}[C_p(T_{hot} - T_0) - T_0(C_p \ln\frac{T_{hot}}{T_0} - R \ln\frac{P_{hot}}{P_0})] + \frac{\dot{m}_{hot} v_{hot}^2}{2} \quad (8)$$

And:

$$\sum \dot{E}_{o,cold} = \dot{m}_{cold}[C_p(T_{cold} - T_0) - T_0(C_p \ln\frac{T_{cold}}{T_0} - R \ln\frac{P_{cold}}{P_0})] + \frac{\dot{m}_{cold} v_{cold}^2}{2} \quad (9)$$

Finally [26]:

$$\sum \dot{E}_{lost} = \dot{E}_i + \dot{E}_o \quad (10)$$

Where, $\sum \dot{E}_{lost}$ are the destroyed exergy. The exergy efficiency can be written as:

$$\eta = \frac{\sum \dot{E}_o}{\sum \dot{E}_i} \quad (11)$$

A complete form of exergy balance in Ranque-Hilsch vortex tube is shown in Fig. 3.

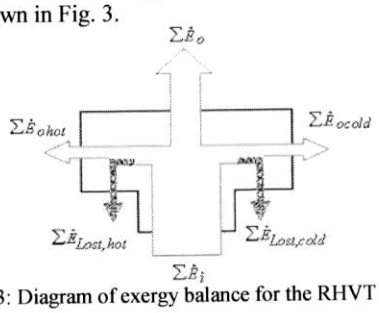

Fig. 3: Diagram of exergy balance for the RHVT system

2. TURBULENCE MODEL DESCRIPTION

In this investigation two turbulence models have been employed. These turbulence models are standard k-ε and standard k-ω. Other models such as Reynolds stress equations and RNG k-ε could not be made to converge yet. But standard k-ε and standard k-ω have good agreement of numerical results with the experimental data. In the vortex tube the compressible turbulent flows are governed by the conservation of mass, momentum and energy equations. The flow field throughout the vortex tube is fully turbulent. About standard k-ε model, the turbulence kinetic energy, k, is obtained from the following transport equation:

$$\frac{\partial}{\partial t}(\rho k)+\frac{\partial}{\partial x_i}(\rho k u_i)=\frac{\partial}{\partial x_j}[(\mu+\frac{\mu_t}{\sigma_k})\frac{\partial k}{\partial x_j}]+G_k+G_b-\rho\varepsilon-Y_M \quad (12)$$

$$\frac{\partial}{\partial t}(\rho\varepsilon)+\frac{\partial}{\partial x_i}(\rho\varepsilon u_i)=\frac{\partial}{\partial x_j}[(\mu+\frac{\mu_t}{\sigma_\varepsilon})\frac{\partial\varepsilon}{\partial x_j}]+C_{1\varepsilon}\frac{\varepsilon}{k}(G_k+C_{3\varepsilon}G_b)-C_{2\varepsilon}\rho\frac{\varepsilon^2}{k} \quad (13)$$

In these equations, G_k, G_b, and Y_M represent the generation of turbulence kinetic energy due to the mean velocity gradients, the generation of turbulence kinetic energy due to buoyancy and the contribution of the fluctuating dilatation in compressible turbulence to the overall dissipation rate, respectively. $C_{1\varepsilon}$ and $C_{2\varepsilon}$ are constants. These default values have been determined from experiments with air and water for fundamental turbulent shear flows including homogeneous shear flows and decaying isotropic grid turbulence. They have been found to work fairly well for a wide range of wall bounded and free shear flows. σ_k and σ_ε are also the turbulent Prandtl numbers for k and ε. The turbulent (or eddy) viscosity, μ_t, is computed as follows:

$$\mu_t = \rho C_\mu \frac{k^2}{\varepsilon} \quad (14)$$

where, C_μ is a constant. The model constants $C_{1\varepsilon}$, $C_{2\varepsilon}$, C_μ, σ_k and σ_ε have the following default values: $C_{1\varepsilon}$ = 1.44, $C_{2\varepsilon}$ = 1.92, C_μ = 0.09, σ_k = 1.0, σ_ε = 1.3. Finite volume method with a 3D structured mesh is applied to the governing equations, which is one of the numerical approaches to describe complex flow patterns in the vortex tube. Inlet air is considered as a compressible working fluid, where its specific heat, thermal conductivity and dynamic viscosity are taken to be constant during the numerical analysis procedure. Second order upwind scheme is utilized to discretize convective terms, and SIMPLE algorithm is used to solve the momentum and energy equations simultaneously.

Now about k-ω model, the turbulence kinetic energy, k, is obtained from the following transport equation:

$$\rho\frac{\partial k}{\partial \tau}+\rho u_j k_{,j}=(\mu+\frac{\mu_\tau}{\sigma_k}k_{,j})_{,j}+G+B-\rho\omega k \quad (15)$$

And for ω:

$$\rho\frac{\partial \omega}{\partial \tau}+\rho u_j \omega_{,j}=(\mu+\frac{\mu_\tau}{\sigma_\omega}\omega_{,j})_{,j}+C_1\frac{\omega}{k}G+C_1(1-C_3)\frac{\omega}{k}B-C_2\rho\omega^2 \quad (16)$$

And turbulent viscosity in k-ω model can be defined as:

$$\mu_t = \rho C_\mu \frac{k^2}{\omega} \quad (17)$$

Where, C_μ is constant. The model constants C_1, C_2, C_μ, σ_k and σ_ω have the following default values: C_1 = 0.555, C_2 = 0.8333, C_μ = 0.09, σ_k = 2, σ_ω = 2.

3. PHYSICAL AND 3D CFD MODEL OF VORTEX TUBE

The FLUENT ™ software package was used to create the CFD model. The created 3D CFD model is based on that was used by Skye *et al* [7]. It is noteworthy that, an Exair™ 708 slpm [27] vortex tube was used by Skye to take all of the experimental data and is shown in Fig. 4.

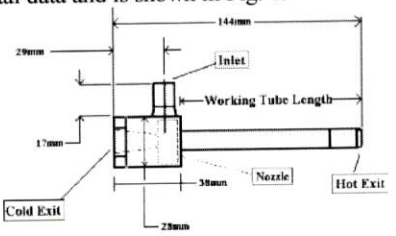

Fig. 4: Schematic of vortex tube that used by Skye *et al.*

A compressible form of the Navier-Stokes equation along with the standard k-ε model and the standard k-ω model by second order upwind for momentum, turbulence and energy equations has been used to simulate the phenomenon of flow pattern and temperature separation ration in a vortex tube with 6 inlet section and the cold and hot exit are axial orifices with areas of 30.2 mm^2 and 95.0 mm^2 respectively. This CFD model is three-dimensional, axisymmetric and steady and employs two turbulence models for its computations. A complete list of model parameters can be found in Table 1.

Table 1 : Geometric measurements of the vortex tube that was used by Skye *et al.* (2006)

Measurement	Value
Working tube length	106 mm
Nozzle height	0.97 mm
Nozzle width	1.41 mm
Nozzle total inlet area (An)	8.2 mm^2
Cold exit diameter	6.2 mm
Cold exit area	30.3 mm^2
Hot exit diameter	11 mm
Hot exit area	95 mm^2

Finally the 3D CFD mesh grid can be shown in Fig. 5. Boundary conditions for this study are based on the experimental investigation by Sky *et al* [7].The inlet is modeled as a mass-flow-inlet .The inlet stagnation temperature and the total mass flow inlet are fixed to 294.2 K and 8.35 *gr/s* respectively. The static pressure at the cold exit boundary was fixed at experimental measurements pressure and is modeled as a pressure-outlet. The static pressure at the hot exit boundary is adjusted in the way to vary the cold mass fraction.

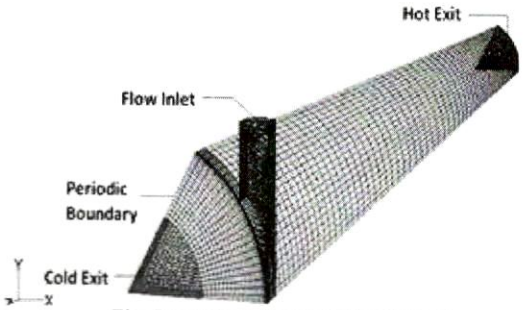

Fig. 5. a sector of computational domain

4. RESULTS AND DISCUSSION

The CFD investigation has been performed for a vortex tube when diameter was 11.4 mm and length of working tube was 106 mm. This vortex tube worked under certain boundary and operating conditions that measured in experimental study by Skye *et al* [7]. Results of this CFD study have been validated with experimental data and there is a comparison between the 3D CFD results of this investigation and the results of Skye *et al* [7] including experimental and 2D CFD results. The model used in this study is three-dimensional but the model used by Skye *et al* [7] in his CFD analysis was two-dimensional which it is the main difference between this work and Skye's study. The Result of this study shows CFD is a powerful tool for prediction the treatment of flows because the obtained results of prediction by the CFD models show good agreement with the experimental data. First, pay attention to results about temperature separation. The temperature separations achieved from this model have been compared with the experimental and computational results of Skye's model. The temperature difference between the gas that escapes from the hot exit and the pressured inlet gas can be defined as hot exit temperature difference (ΔT_h) and the predicted results by 3D CFD model shows good agreement with the experimental results. This prediction is compared with experimental data for validation and has been shown as a function of cold mass fraction in Fig. 6. Figure 6 shows the result of this numerical study is a good prediction in thermal field. This figure indicates CFD is a powerful tool for prediction of flow treatment. According to Fig. 6, the hot exit temperature difference (ΔT_h) is observed to increase with an increase in the cold mass fraction.

The results of this study show the prediction of the 3D CFD model about the cold exit temperature difference (ΔT_c), lies between the experimental and computational results of Skye *et al* [7]. As seen in Fig. 7, the general shape of CFD cold temperature difference (ΔT_c) curve is similar to the experimental curve of ΔT_c. Figure 7 shows, thermal prediction of standard k-ε model in this case is better than thermal prediction of standard k-ω model. In Figure 7, the maximum cold temperature difference in the standard k-ε model curve occurs in cold mass fraction range of 0.36-0.5. Variation of temperature difference between the gas that escapes from the cold exit and gas that exits from the hot exhaust, (ΔT), can be found in Fig. 8. As seen in Figure 8, the temperature difference between the cold and hot exit (ΔT) predicted by standard k-ε turbulence model in the three-dimensional CFD model is in good agreement with experimental results. According to Fig. 8, ΔT increases with an increase in the cold mass fraction similar to the treatment of ΔT_h curve. The maximum temperature difference of 99.94K was found due to a cold mass fraction of 0.8214. In according to Figure 6, 7 and 8, the standard k-ε model has better thermal conclusions in comparison with the standard k-ω model in this case.

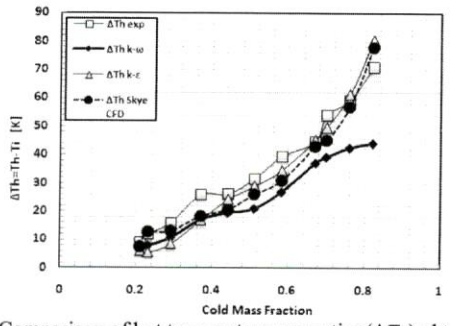

Fig. 6 : Comparison of hot temperature separation(ΔT_h) obtained at present 3D CFD model and Skye *et al.* (2006) simulation(2D) and experiments as a function of cold mass fraction

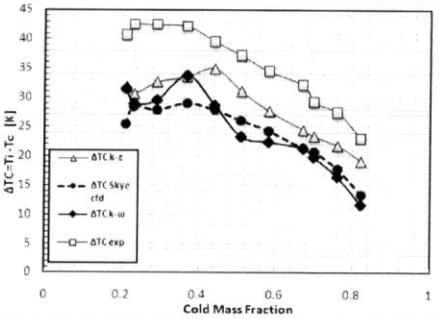

Fig. 7 : Comparison of cold temperature separation (ΔT_c)obtained at present 3D CFD model and Skye *et al.* (2006) simulation(2D) and experiments as a function of cold mass fraction

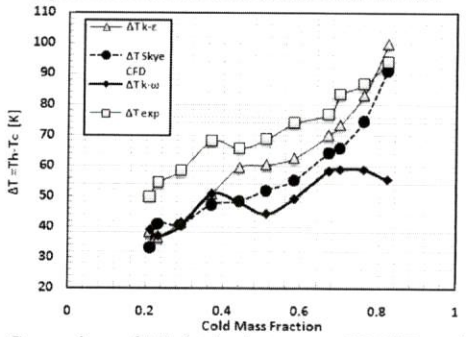

Fig. 8: Comparison of ΔT obtained at present 3D CFD model and experimentally measured ΔT and ΔT predicted by 2D CFD model as a function of cold mass fraction. 2D simulation and experimental work has been carried out by Skye *et al.* (2006)

The gradient of total temperature has been described in Fig. 9.This contours shows that the minimum total temperature occurs in the central region of working tube. Figure 10

illustrates the contours of static temperature across the working tube. A comparison between Fig. 9 and Fig. 10 indicates the static temperature variations across the working tube are considerably smaller than those found for the total temperature.

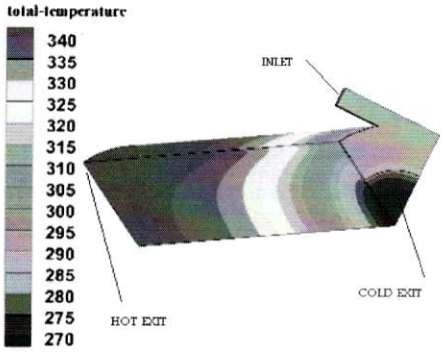

Fig. 9: Contours of total temperature

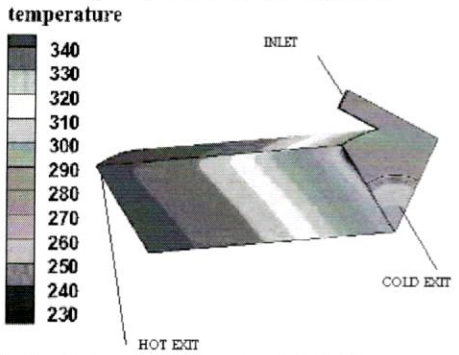

Fig. 10: Contours of temperature (Static Temperature)

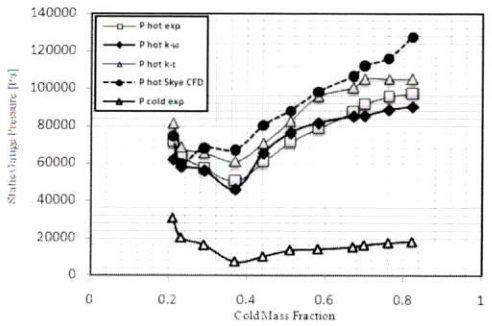

Fig. 11: Comparison of static hot gauge pressure (P_h) obtained at present 3D CFD model and Skye *et al.* (2006) simulation(2D) and experiments as a function of cold mass fraction

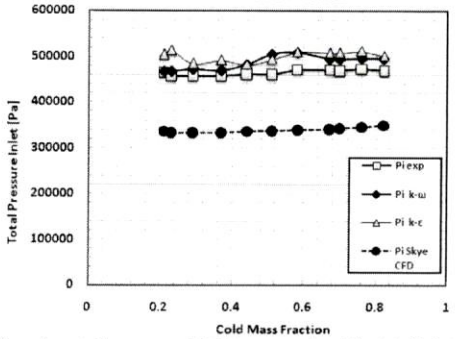

Fig. 12: Experimentally measured inlet pressured and the total inlet pressure (P_i) predicted by 2D (Skye) and 3D (This Study) CFD models as a function of cold mass fraction

Figure 11 shows the variation of static pressure at the hot exit as a function of cold mass fraction. In the CFD model, the cold exit pressure boundary condition was specified at the measured cold exit pressure. Figure 11, shows the minimum pressure of cold and hot exit occurs due to a cold mass fraction of 0.3691. This fact is clearly observable that the pressure analysis of standard k-ε model has less accuracy in comparison with standard k-ω model, this means that, the standard k-ω model has the better conclusions in the pressure computations and its results are in good agreement with the experimental data. In Figure 12 we have the variation of total inlet pressure as a function of cold mass fraction. This validation shows the results of three-dimensional CFD model are better than the results of two-dimensional CFD model of Skye *et al* [7].

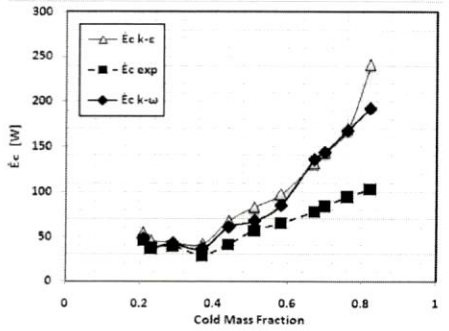

Fig. 13: The total cold exergy ($\dot{E}_c$) for different turbulence models and comparison with experimental results

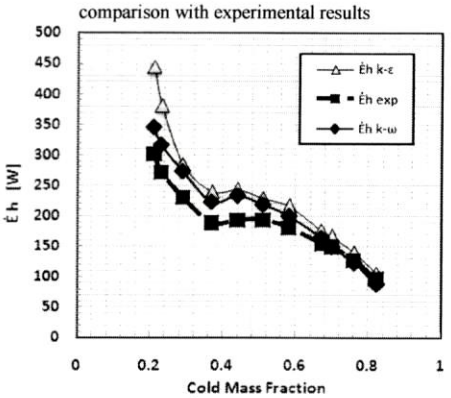

Fig. 14: The total hot exergy ($\dot{E}_h$) for different turbulence models and comparison with experimental results

About exergy analysis of this study, Fig. 13 shows the total exergy of cold outlet as a function of cold mass fraction. The total exergy of cold outlet is observed to increase with an increase in the cold mass fraction. The minimum cold exergy occurs in the cold mass fraction of 0.3691. Figure 13 indicated this fact that the procedure of CFD model in the calculation and prediction of features of fluids is a reliable procedure. The variation of total exergy of hot outlet gas is shown in Figure 14. The total exergy of hot outlet as a function of cold mass fraction is observed to decrease with an increase in the cold mass fraction. About the exergy analysis in this investigation it is visible that the standard k-ω model has the conclusions with good accuracy and its results are close to the experimental data. Now there is a figure that shows the total lost exergy for different values of the cold mass fraction. In Figure 15, the maximum lost exergy is occurred in the cold mass fraction of 0.3691. The minimum lost exergy occurs in the cold mass fraction of 0.21. In cold mass fraction range of 0.21-0.3691, the lost exergy is

observed to increase with increase in the cold mass fraction. In Figure 16, the variation of the total inlet exergy is visible. However the total inlet exergy approximately has a constant and stable value as shown in Fig.16. Finally, the curves of exergy efficiency obtained from the 3D CFD model as a function of cold mass fraction has been illustrated in a comparison form with the experimental curve in Fig. 17. The maximum exergy efficiency occurs in the cold mass fraction of 0.21. With increasing the amount of cold mass fraction in range of 0.21-0.3691, the exergy efficiency is observed to decrease. In the cold mass fraction of 0.3691 we have the minimum exergy efficiency in the CFD turbulence models.

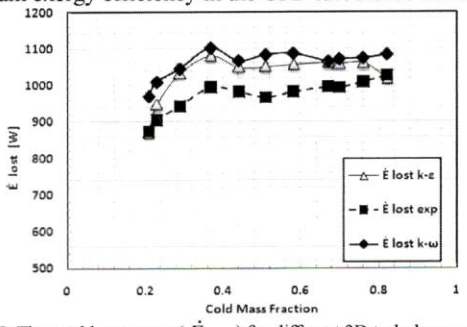

Fig. 15: The total lost exergy ($\dot{E}_{Lost}$) for different 3D turbulence models and comparison with experimental results

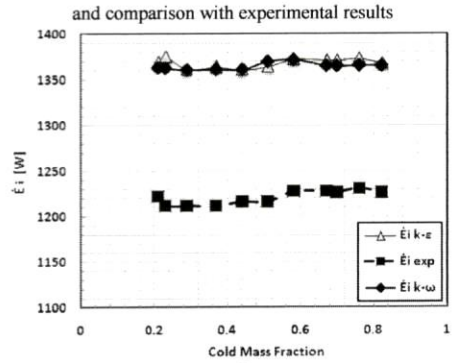

Fig. 16: The total inlet exergy ($\dot{E}_i$) for different 3D turbulence models and comparison with experimental results

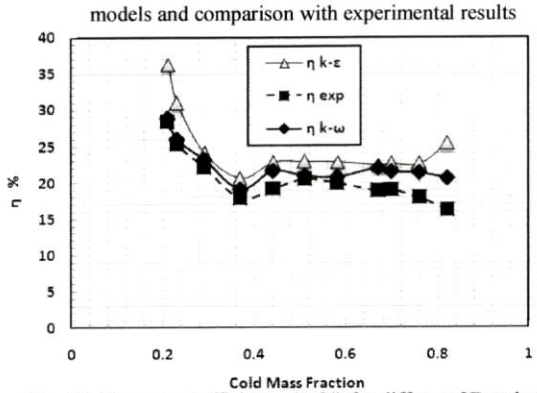

Fig. 17: The exergy efficiency (ŋ, %) for different 3D turbulence models and comparison with experimental results

5. CONCLUSIONS

In this numerical study, the case study was a vortex tube which worked under the certain boundary and operating conditions. These conditions were determined in an experimental study by Skye *et al.* (2006). The conclusions and results of experimental study were applied to carry out the CFD analysis. The 3D CFD model has been created and CFD computations were based on two turbulence models. These models contain standard k-ω model and standard k-ε model. The results achieved from this analysis, such as variation of exergy, temperature and pressure have been shown in figures. The temperature figures shows the CFD curves are in good agreement with experimental data. ΔT_h is observed to increase with an increase in the cold mass fraction and maximum ΔT_c occurs in cold mass fraction range of 0.36-0.5. Treatment of ΔT curve is an ascending procedure as a function of cold mass fraction. As seen in the pressure figures, in the cold mass fraction of 0.3691, the static pressure of cold and hot exit is minimal. In prediction of fluid temperature in difference cold mass fraction, standard k-ε model has good results that are in good agreement with experimental data. According to Figure 6, 7 and 8, the standard k-ε model has better thermal conclusions in comparison with the standard k-ω model in this case. This means that in thermal prediction, standard k-ε model is better than standard k-ω model in this case. But as seen in the pressure figures (Figure 11, 12 and 13), the prediction results of standard k-ω model are closer than the prediction results of standard k-ε model to the experimental data in pressure field. Finally the maximum lost exergy occurs at a cold mass fraction of 0.3691. When the cold mass fraction reaches to 0.3691, we have a minimum value of pressure at cold and hot exit. Consequently, the lost exergy is maximal when the pressure of outlets reaches to minimum value. The maximum exergy efficiency of this case occurs in a cold mass fraction of 0.21 that is approved by the experimental results.

6. REFERENCES

1. G. J. Ranque, Experiments on expansion in a vortex with simultaneous exhaust of hot air and cold air, *Le Journal de Physique et le Radium*, vol. 4, pp. 112-114, 1933
2. R. Hilsch, The use of expansion of gases in a centrifugal field as a cooling process, *Rev. Sci. Instrum*, vol. 18, pp. 108-113, 1947.
3. S. E. Rafiee and M. Rahimi, Experimental study and three-dimensional (3D) computational fluid dynamics (CFD) analysis on the effect of the convergence ratio, pressure inlet and number of nozzle intake on vortex tube performance-Validation and CFD optimization, *Energy*, vol. 63, pp. 195-204, 2013.
4. B. K. Ahlborn and J.M. Gordon, The vortex tube as a classic thermodynamic refrigeration cycle, *Journal of Applied Physics*, vol. 88, pp. 3645-3653, 2000
5. K. Stephan, S. Lin, M. Durst, F. Huang, D. Seher, An investigation of energy separation in a vortex tube, *Int. J. Heat Mass Transfer*, vol. 26, pp. 341-348, 1983
6. S. E. Rafiee, M. M. Sadeghiazad, Three-dimensional and Experimental investigation on the effect of cone length of throttle valve on thermal performance of a vortex tube using k-ε turbulence model, *Applied Thermal Engineering*, vol. 66, pp. 65-74, 2014.
7. H. M. Skye, G. F. Nellis, S. A. Klein, Comparison of CFD analysis to empirical data in a commercial vortex tube, *Int. J. Refrig*, vol. 29, pp. 71-80, 2006
8. N. Pourmahmoud, A. Hassanzadeh, S. E. Rafiee, M. Rahimi, Three Dimensional Numerical Investigation of Effect of Convergent Nozzles on the Energy Separation in a Vortex Tube, *International Journal of Heat and Technology*, vol. 30(2), pp. 133-140, 2012

9. S. E. Rafiee, M. Rahimi, N. Pourmahmoud, Three-dimensional numerical investigation on a commercial vortex tube based on an experimental model- Part I: Optimization of the working tube radius, *International Journal of Heat and Technology*, vol. 31(1), pp. 49-56, 2013
10. N. Pourmahmoud, S. E. Rafiee, M. Rahimi, A. Hasanzadeh, Numerical energy separation analysis on the commercial Ranque-Hilsch vortex tube on basis of application of different gases, *Scientia Iranica*, vol. 20(5), pp. 1528-1537, 2013.
11. H. S. Chang, Experimental and Numerical Studies in a Vortex Tube. *Journal of Mechanical Science and Technology* Vol 20(3), pp. 418-425, 2006
12. M. Ameri, B. Behnia, The study of key design parameters effects on the vortex tube performance, *Journal of Thermal Science*, vol. 18(4), pp. 370-376, 2010.
13. Eisma and S. Promvonge, Numerical investigations of the thermal separation in a Ranque-Hilsch vortex tube. *Int J Heat Mass Transfer*, vol(50), pp. 821-32, 2007.
14. A. B. Agrawal, V. Shrivastava, Retrofitting of vapour compression refrigeration trainer by an eco-friendly refrigerant, *Indian J. Sci. Technol*, vol. 3(4), 2010.
15. B. Jayaraman, P. Senthil Kumar. Design, optimization and performance analysis of orifice pulse tube cryogenic refrigerators. *Indian J. Sci. Technol*, vol. 3(4), 2010
16. V. Kirmaci, Optimization of counter flow Ranque-Hilsch vortex tube performance using Taguchi method. *International Journal of Refrigeration*, vol. 32, pp. 1487-1494, 2009
17. K. Dincer , A. Avci, S. Baskaya, A. Berber, Experimental investigation and exergy analysis of the performance of a counter flow Ranque-Hilsch vortex tube with regard to nozzle cross-section areas. *Int. J. Refrig*, vol. 33, pp. 954-962, 2010
18. I. Ceylan, M. Aktas, H. Dogan, Energy and exergy analysis of timber dryer assisted heat pump, *Applied Thermal Engineering*, vol. 27, pp. 216-222, 2007
19. V. Kirmaci, Exergy analysis and performance of a counter flow Ranque-Hilsch vortex tube having various nozzle numbers at different inlet pressures of oxygen and air. *International Journal of Refrigeration*, vol. 32, pp. 1626-1633, 2009
20. O. Ozgener, A. Hepbasli, A review on the energy and exergy analysis of solar assisted heat pump systems. *Renewable and Sustainable Energy Reviews*, vol. 11, pp. 482-496, 2007.
21. R. Saidur, M.A. Sattar, H.H. Masjuki, H. Abdessalam, B. S. Shahruan, Energy and exergy analysis at the utility and commercial sectors of Malaysia, *Energy Policy*, vol. 35, pp. 1956-1966, 2007
22. H. Esen, M. Inalli, M. Esen, K. Pihtili, Energy and exergy analysis of a ground-coupled heat pump system with two horizontal ground heat exchangers, *Building and Environment*, vol. 42, pp. 3606-3615, 2007
23. E.Lorenzini, M.Spiga, Aspetti fluidodinamici della separazione isotopica mediante tubi a vortice di Hilsch Ingegneria, n. 5-6, pp. 121-126 (maggio-giugno 1982).
24. E.K. Akpinar, A. Hepbasli, A comparative study on exergetic assessment of two ground-source (geothermal) heat pump systems for residential applications, *Building and Environment*, vol. 42, pp. 2004-2013, 2007
25. T.J. Kotas, The Exergy Method of Thermal Plant Analysis, *Anchor Brendon Ltd*, Tiptree, Essex, 1985
26. K. Dincer, S. Baskaya, Assessment of plug angle effect on exergy efficiency of counter flow Ranque-Hilsch vortex tubes with the exergy analysis method, *Journal of the Faculty of Engineering and Architecture of Gazi University*, vol. 24, pp. 533-538, 2009
27. Exair Corporation. Vortex tubes and spot cooling products. Available at [http://www.exair.com]
28. S. Eiamsa-ard, P. Promvonge, Review of Ranque-Hilsch effects in vortex tubes, *Renewable and Sustainable Energy Reviews*, vol. 12, pp.1822-1842. 2007